

DIVERSE KINEMATIC SIGNATURES FROM REVERBERATION MAPPING OF THE BROAD-LINE REGION IN ACTIVE GALACTIC NUCLEI

K. D. DENNEY¹, B. M. PETERSON^{1,2}, R. W. POGGE^{1,2}, A. ADAIR³, D. W. ATLEE¹, K. AU-YONG³, M. C. BENTZ^{1,4}, J. C. BIRD¹, D. J. BROKOFKY^{5,6}, E. CHISHOLM³, M. L. COMINS^{1,7}, M. DIETRICH¹, V. T. DOROSHENKO^{8,9,10}, J. D. EASTMAN¹, Y. S. EFIMOV⁹, S. EWALD³, S. FERBEY³, C. M. GASKELL^{5,11}, C. H. HEDRICK^{5,7}, K. JACKSON³, S. A. KLIMANOV^{9,10}, E. S. KLIMEK^{5,12}, A. K. KRUSE^{5,13}, A. LADÉROUTE³, J. B. LAMB¹⁴, K. LEIGHLY¹⁵, T. MINEZAKI¹⁶, S. V. NAZAROV^{9,10}, C. A. ONKEN^{17,18}, E. A. PETERSEN⁵, P. PETERSON¹⁹, S. POINDEXTER¹, Y. SAKATA²⁰, K. J. SCHLESINGER¹, S. G. SERGEEV^{9,10}, N. SKOLSKI³, L. STIEGLITZ³, J. J. TOBIN¹⁴, C. UNTERBORN¹, M. VESTERGAARD^{21,22}, A. E. WATKINS⁵, L. C. WATSON¹, AND Y. YOSHII¹⁶

(Accepted 2009 September 15)
Draft version October 25, 2018

ABSTRACT

A detailed analysis of the data from a high sampling rate, multi-month reverberation mapping campaign, undertaken primarily at MDM Observatory with supporting observations from telescopes around the world, reveals that the H β emission region within the broad line regions (BLRs) of several nearby AGNs exhibit a variety of kinematic behaviors. While the primary goal of this campaign was to obtain either new or improved H β reverberation lag measurements for several relatively low luminosity AGNs, we were also able to unambiguously reconstruct velocity-resolved reverberation signals from a subset of our targets. Through high cadence spectroscopic monitoring of the optical continuum and broad H β emission line variations observed in the nuclear regions of NGC 3227, NGC 3516, and NGC 5548, we clearly see evidence for outflowing, infalling, and virialized BLR gas motions, respectively.

Subject headings: galaxies: active — galaxies: nuclei — galaxies: Seyfert

1. INTRODUCTION

Reverberation mapping (Blandford & McKee 1982; Peterson 1993) is a technique applied to spectroscopic observations of type 1 AGNs to infer properties of the broad line-emitting region (BLR) through characterizations of time delays between continuum and broad emission-line flux variations. This method has become extremely useful and quite successful in its current application of directly measuring BLR radii and black hole masses (M_{BH}). However, the fundamental objective of reverberation mapping, as its name implies, is to reconstruct or map the emissivity and velocity distribution of the BLR line-emitting gas as a function of position as it ‘reverberates’ in response to the flux variations of the ionizing continuum. Because the position of the gas can be inferred through the emission-line time delay, τ ($R_{\text{BLR}} = c\tau$), the resulting reconstruction is called a velocity–delay map (see Horne et al. 2004) and is the best means, with current technology, to obtain direct knowledge about the geometry and kinematics of the BLR.

Past attempts at producing velocity–delay maps (e.g.,

Canada, 5071 West Saanich Road, Victoria, BC V9E 2E7, Canada
¹⁸ Current address: Mount Stromlo Observatory, Research School of Astronomy & Astrophysics, The Australian National University, Cotter Road, Weston Creek, ACT 2611, Australia; onken@mso.anu.edu.au

¹⁹ Ohio University, Department of Physics and Astronomy, Athens, OH 45701-2979, USA

²⁰ Department of Astronomy, School of Science, University of Tokyo, 7-3-1 Hongo, Bunkyo-ku, Tokyo 113-0013, Japan

²¹ Steward Observatory, The University of Arizona, 933 North Cherry Avenue, Tucson, AZ 85721, USA

²² DARK Cosmology Centre, Niels Bohr Institute, Copenhagen University

¹ Department of Astronomy, The Ohio State University, 140 West 18th Avenue, Columbus, OH 43210, USA; denney, peterson, pogge@astronomy.ohio-state.edu

² Center for Cosmology and AstroParticle Physics, The Ohio State University, 191 West Woodruff Avenue, Columbus, OH 43210, USA

³ Centre of the Universe, Herzberg Institute of Astrophysics, National Research Council of Canada, 5071 West Saanich Road, Victoria, BC V9E 2E7, Canada

⁴ Present address: Department of Physics and Astronomy, 4129 Frederick Reines Hall, University of California at Irvine, Irvine, CA 92697-4575, USA; mbentz@uci.edu

⁵ Department of Physics & Astronomy, University of Nebraska, Lincoln, NE 68588-0111, USA.

⁶ Deceased, 2008 September 13

⁷ Current address: Astronomy and Astrophysics Department, Pennsylvania State University, 525 Davey Laboratory, University Park, PA 16802, USA

⁸ Crimean Laboratory of the Sternberg Astronomical Institute, p/o Nauchny, 98409 Crimea, Ukraine; vdorosh@sai.crimea.ua

⁹ Crimean Astrophysical Observatory, p/o Nauchny, 98409 Crimea, Ukraine; sergeev, efim@crao.crimea.ua, serg-dave2004@mail.ru, nazarastron2002@mail.ru

¹⁰ Isaak Newton Institute of Chile, Crimean Branch, Ukraine

¹¹ Current address: Astronomy Department, University of Texas, Austin, TX 78712-0259, USA; gaskell@astro.as.utexas.edu

¹² Current address: Astronomy Department, MSC 4500, New Mexico State University, PO BOX 30001, La Cruces, NM 88003-8001, USA

¹³ Current address: Physics Department, University of Wisconsin-Madison, 1150 University Avenue, Madison, WI 53706-1390, USA

¹⁴ Department of Astronomy, University of Michigan, 500 Church St., Ann Arbor, MI 48109-1040, USA

¹⁵ Homer L. Dodge Department of Physics and Astronomy, The University of Oklahoma, 440 W. Brooks St., Norman, OK 73019, USA

¹⁶ Institute of Astronomy, School of Science, University of Tokyo, 2-21-1 Osawa, Mitaka, Tokyo 181-0015, Japan; minezaki, yoshii@ioa.s.u-tokyo.ac.jp

¹⁷ Plaskett Fellow; Dominion Astrophysical Observatory, Herzberg Institute of Astrophysics, National Research Council of

Done & Krolik 1996; Ulrich & Horne 1996; Kollatschny 2003) have not yielded completely satisfactory results, primarily on account of limitations in temporal sampling, with inadequate time resolution or campaign duration or both. Even given these limitations, previous studies have successfully measured time delays and black hole masses in over 40 type 1 AGNs (see e.g., Peterson et al. 2004; Bentz et al. 2009). In addition, basic investigations into time delay differences between multiple emission lines have shown that the BLR is virialized across broad line-emitting regions of different species (e.g., Peterson et al. 2004, and references therein). Other studies of the velocity dependence of the lag across a single emission line region have shown suggestive evidence that the BLR commonly contains a radial inflow component in addition to circular motions (e.g., Gaskell 1988; Crenshaw & Blackwell 1990; Koratkar & Gaskell 1991; Done & Krolik 1996).

The experiences from earlier reverberation programs have led to more recent campaigns that address the main observational obstacles encountered in the past — relative sampling rate, campaign duration, and data quality. Consequently, there has been consistent success in measuring BLR radii in new targets and remeasuring radii that now supersede previous, lower-precision or ambiguous measurements due to inadequate time-sampling (e.g., Denney et al. 2006; Bentz et al. 2006; Grier et al. 2008; Denney et al. 2009, hereafter D09a). Furthermore, these campaigns enable statistically significant detections of reverberation signals at higher velocity resolutions than have previously been found due mainly to the data restrictions discussed above. For example, Bentz et al. (2008) revealed a clear signal of radial inflow within the $H\beta$ emission region of the BLR in Arp 151, and Bentz et al. (2009) show further evidence for distinct kinematic behavior in at least one other AGN from the same program (the Lick AGN Monitoring Project). Here we report on results of our own recent high time-resolution monitoring program undertaken at five observatories. The first results of this program have already been published (D09a), and additional results are in preparation (K. D. Denney et al. 2009, in preparation, hereafter D09b). In this Letter, we present the most clear velocity-resolved reverberation signals recovered from this campaign. Our results highlight three distinctly different BLR kinematic signatures — inflow, outflow, and virialized motions — for three separate targets — NGC 3227, NGC 3516, and NGC 5548, respectively. These results reveal kinematic diversity in reverberation signals and underscore the importance of higher time resolution spectral monitoring. This represents an important step between measuring average BLR response times and black hole masses to realizing the full potential of this technique through the recovery of a velocity–delay map.

2. OBSERVATIONS AND DATA ANALYSIS

Spectra of the nuclear regions of NGC 3227, NGC 3516, and NGC 5548 were obtained from a combination of the 1.3 m telescope at MDM Observatory, the 2.6 m Shajn telescope of the Crimean Astrophysical Observatory (CrAO), and the Plaskett 1.8 m telescope at Dominion Astrophysical Observatory (DAO). Spectroscopic observations targeted the $H\beta$ $\lambda 4861$ and $[O\text{ III}]\lambda\lambda 4959, 5007$

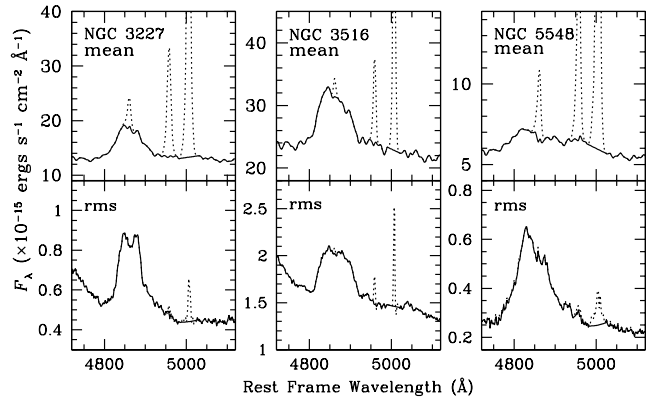


FIG. 1.— Mean and rms spectra of NGC 3227 (left), NGC 3516 (middle), and NGC 5548 (right) from MDM observations. The solid line shows the mean and rms spectrum formed after removal of the $[O\text{ III}]\lambda\lambda 4959, 5007$ narrow emission lines, and the dotted lines represent the spectra prior to this subtraction (note the small residuals in the rms spectra).

emission line region of the optical spectrum. The top panels of Figure 1 show the mean spectrum of each of the three targets based on the MDM observations, and the bottom panels show only the variable emission in the form of an rms spectrum for each object, respectively. Emission line light curves were made from the integrated $H\beta$ flux measured above a linearly interpolated continuum fit to the MDM, CrAO, and DAO spectra.

In addition to spectral observations, we obtained supplemental V -band photometry from the 2.0-m Multicolor Active Galactic Nuclei Monitoring (MAGNUM) telescope at the Haleakala Observatories in Hawaii (Yoshii 2002; Yoshii et al. 2003), the 70-cm telescope of the CrAO, and the 0.4-m telescope of the University of Nebraska (UNebr.). Continuum light curves were created with observations from each V -band photometric data set and the average continuum flux density near rest frame ~ 5100 Å in each spectrum of the spectroscopic data sets. The reader is referred to D09a and D09b for details describing campaign observing setups and data reduction, flux calibration of the spectra, and intercalibration of the data sets to form the single set of optical continuum and $H\beta$ emission line light curves shown for each object in Figure 2.

Table 1 displays basic statistical parameters describing the final light curves shown in Figure 2. Column 1 gives the object, and Column 2 lists the spectral feature represented by each light curve. The number of data points in each light curve is shown in Column 3, with the median sampling interval between these data points given in Column 4. Column 5 shows the mean fractional error in the fluxes of each time series. Column 6 gives the excess variance, calculated as

$$F_{\text{var}} = \frac{\sqrt{\sigma^2 - \delta^2}}{\langle f \rangle} \quad (1)$$

where σ^2 is the variance of the observed fluxes, δ^2 is their mean square uncertainty, and $\langle f \rangle$ is the mean of the observed fluxes (Rodríguez-Pascual et al. 1997). Column 7 is the ratio of the maximum to minimum flux in the light curves, and Column 8 gives the adopted mean $H\beta$ time lag and uncertainties determined through the primary time series analysis which utilized the full $H\beta$ line profile

TABLE 1
LIGHT CURVE STATISTICS AND MEAN H β LAGS

Object (1)	Time Series (2)	N (3)	T_{median} (days) (4)	Frac. Err (5)	Mean F_{var} (6)	R_{max} (7)	τ_{cent} (days) (8)
NGC 3227	5100 Å	171	0.45	0.03	0.10	1.9 ± 0.1	...
	H β	75	1.00	0.03	0.08	1.5 ± 0.1	3.8 ± 0.8
NGC 3516	5100 Å	198	0.54	0.06	0.28	5.9 ± 1.5	...
	H β	93	1.00	0.04	0.15	1.9 ± 0.2	$11.7^{+1.0}_{-1.5}$
NGC 5548	5100 Å	182	0.56	0.03	0.11	1.7 ± 0.1	...
	H β	108	1.00	0.09	0.26	3.7 ± 0.5	$12.4^{+2.7}_{-3.9}$

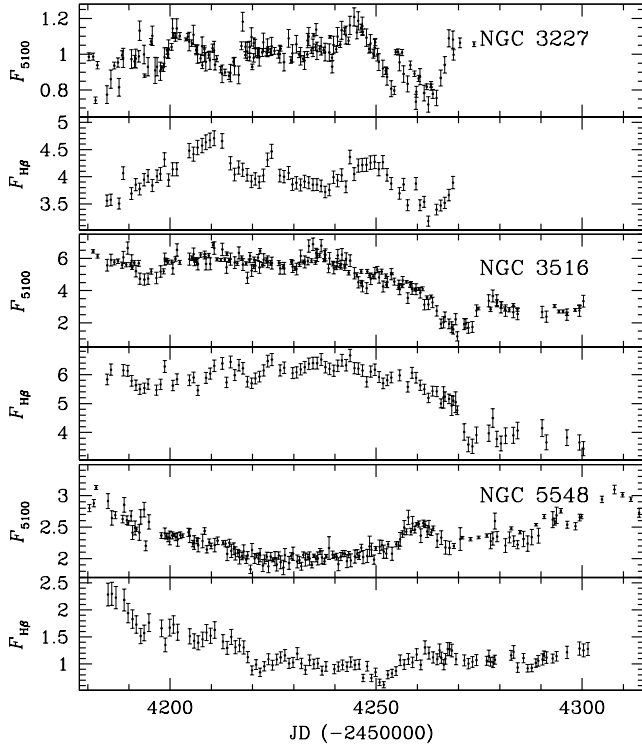


FIG. 2.— Final light curves, after merging all data sets, of the 5100 Å continuum (top panels) and broad H β emission line flux (bottom panels) in units of $10^{-15} \text{ erg s}^{-1} \text{ cm}^{-2} \text{ \AA}^{-1}$ and $10^{-13} \text{ erg s}^{-1} \text{ cm}^{-2}$, respectively, for NGC 3227 (top), NGC 3516 (middle), and NGC 5548 (bottom). Except for the continuum flux scale of NGC 3227, which is arbitrary because a linear fit to long-term secular trends has been divided out, the flux scales reflect all relative and absolute flux calibrations described by D09b.

and is described in detail for each object by D09b.

3. VELOCITY-RESOLVED TIME SERIES ANALYSIS

The lag measurements between the continuum and H β emission listed in Table 1 represent the average time delay across the BLR, measured from the centroid of the cross correlation function (see Peterson et al. 1998, and references therein) produced during the time series analysis of the continuum and full H β line profile light curves shown in Figure 2 (see D09a for details). Here, we focus on the velocity-resolved time series analysis we performed on each target to investigate the potential for recovering velocity-dependent time delays across the H β emission line in order to infer the kinematic structure of the line emitting gas.

We divided the H β emission line into eight velocity-

space bins, whose boundaries were determined by the division of the rms spectrum of each object into eight bins of equal flux, as depicted in the top panels of Figure 3. Compared to the line boundaries used for the full profile analysis leading to the light curves shown in Figure 2, those used for this analysis were slightly narrowed in the cases of NGC 3516 and NGC 3227 in order to include only the most variable portions of the line profile, and boundaries were broadened for NGC 5548 because the rms spectrum shows variability in the red H β wing that extends beneath the [O III] $\lambda 4959$ narrow emission line.

Light curves were created from measurements of the integrated H β flux in each bin and then cross correlated with the continuum light curves shown in Figure 2. The bottom panels of Figure 3 show the lag measurements for each of these bins. Error bars in the velocity direction represent the bin width. The evidence for a velocity-stratified BLR response to continuum variations is clear in all three cases. Interestingly, each case demonstrates a different kinematic signature: (1) outflow is indicated in NGC 3227, given the generally longer lags from red-shifted BLR gas compared to the gas on the blue-shifted side of the line, (2) NGC 3516 shows the opposite signature, with the blue side of the line lagging the red side — an indication that there is an infall component to the gas in this region, similar to that observed in Arp 151 by Bentz et al. (2008), and (3) NGC 5548 shows no radial gas motions, with relatively symmetric lags measurements extending to equally large velocities on both the red and blue sides of line — a clear indication of virialized gas motions, with the high-velocity line wings arising in gas closest to the central source (see Robinson & Perez 1990; Welsh & Horne 1991; Perez et al. 1992; Bentz et al. 2009 for examples of how velocity resolved responses can be related to different BLR geometries; see Peterson (2001) for a related tutorial).

4. DISCUSSION

The velocity-resolved reverberation signals exhibited by the H β -emitting gas in the BLR of these three sources show striking differences in kinematic behavior. This is of particular interest because black hole masses derived from reverberation mapping are only valid under the assumption of gravitational domination of the BLR gas dynamics by the black hole. The influence of gravity on the BLR in NGC 3516 and NGC 5548 is evidenced by the signatures of an infalling gas component in the former and a lack of significant radial motions of any kind in the latter (see Figure 3). The apparent evidence for outflow

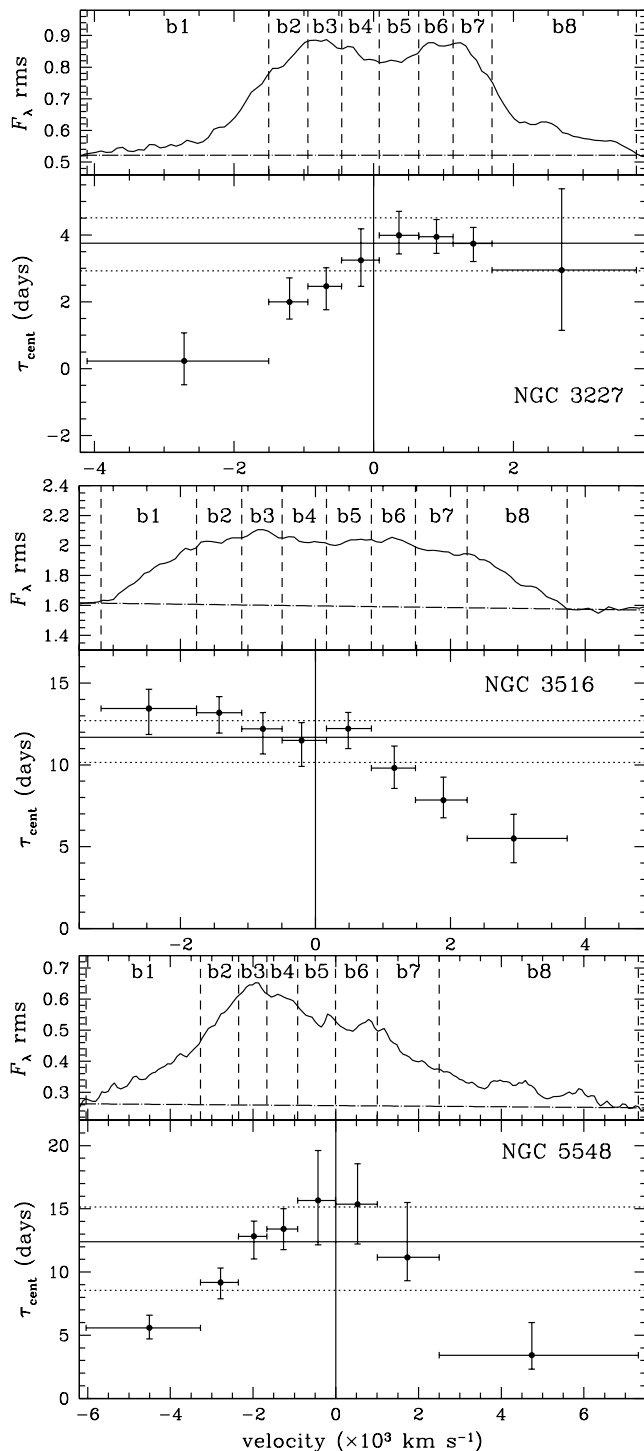


FIG. 3.— Division of the $H\beta$ rms spectral profile into equal-flux bins (top panels; vertical dashed lines), and corresponding velocity-resolved time-delay measurements (bottom panels) for NGC 3227 (top), NGC 3516 (middle), and NGC 5548 (bottom), where the delays are plotted at the flux centroid of each velocity bin. Error bars on the lag measurements in the velocity direction (bottom panels) reflect the bin size, with each bin labeled by number in the top panels and negative velocities referring to blueshifts from the line center and positive velocities redshifts. Error bars on the lag measurements are determined similarly to those for the mean BLR lag (Peterson et al. 1998 with modifications described by Peterson et al. 2004). The horizontal solid and dotted lines in the bottom panel show the mean BLR lag and associated errors, as listed in Table 1, while the horizontal dotted-dashed line in the top panel represents the linearly-fit continuum level. Flux units are the same as in Fig. 1.

in the case of NGC 3227 is a first for reverberation mapping. In some sense, this should be no surprise given the overwhelming evidence for large-scale mass loss from the inner regions of AGNs (Crenshaw, Kraemer, & George 2003). On the other hand, this does call into question the assumptions that allow us to estimate the mass of the central object, though we do hasten to point out that an outflow at escape velocity would still allow us to measure the black hole mass with the levels of accuracy currently claimed. Furthermore, the black hole mass we calculate for NGC 3227 of $M_{\text{BH}} = (7.6^{+1.6}_{-1.7}) \times 10^6 M_{\odot}$, based on the lag in Table 1 and the line dispersion of the broad $H\beta$ line measured from the rms spectrum (see D09b), is consistent within the statistical and systematic uncertainties in this method to independent measurements using galactic stellar (Davies et al. 2006) and gas (Hicks & Malkan 2008) dynamics. We also note that while the $H\beta$ emission line is blueward asymmetric, the $H\beta$ profiles of NGC 3516 and NGC 5548 are even more so, so we ascribe little importance to this. It strikes us as likely that we are observing a complex system such as a two-component BLR, in which there is an outflowing wind, in addition to a virialized, disk component (Murray & Chiang 1997; Eracleous & Halpern 2003). In this case, the mean lag that we measure, which is tracing the position of the majority of the line-emitting gas, arises from the disk component and is therefore under the gravitational influence of the black hole. Meanwhile, the high-velocity, blueshifted emission with very short lags arises from a wind at the inner BLR. Additional support for this scenario comes from the double-peaked profile shape of the rms spectrum, suggesting a disk-like origin (e.g., Eracleous & Halpern 1994). A further test for the virial nature of the BLR in NGC 3227 is to search for reverberation signals from multiple emission lines in this object. Data from this same campaign suggest that the $\text{He II } \lambda 4686$ emission-line flux also varied significantly over the course of the campaign, and future work is planned to search for a reverberation signal from this variable line emission.

The observations of virial motions in NGC 5548 and the outflow in NGC 3227, in particular, are of further interest in the context of comparisons with previous velocity-resolved studies of a similar nature (e.g., Sergeev et al. 1999; Doroshenko et al. 2008). These are largely focused on NGC 5548 (the object for which we have the most reverberation mapping data), and a comprehensive summary of many of these past studies is given by Gaskell & Goosmann (2008), who discuss the support for infalling BLR gas as implied by these various results, particularly for low-ionization lines like $H\beta$. This is in contrast to what we clearly see in NGC 5548 and NGC 3227. It is entirely possible that the velocity fields in these regions could change as a function of accretion rate, luminosity state, or over dynamical timescales. Interpretation of these new results is problematic and probably will remain so with only a handful of examples at single epochs. At this point, generalizing from these few sources is premature.

5. SUMMARY

In this work, we have presented three clear cases of differing velocity signatures of $H\beta$ -emitting gas from the BLR of three nearby AGNs, demonstrating the diversity

and probable complexity of the kinematics in this region. Our ability with this work and that of Bentz et al. (2009, see also Bentz et al. 2008) to recover statistically significant velocity-resolved reverberation responses for multiple objects is principally due to successful completion of campaigns in which high quality, homogeneous observations were obtained over long durations (i.e., multiples of the reverberation lags) with a sampling rate that was high compared to the relevant timescales being investigated. Velocity-resolved reverberation mapping studies such as described here are the next step toward producing a velocity–delay map, which will reconstruct the two-dimensional kinematic structure of the BLR. This, in turn, will allow further insight into the geometry and dynamics of the BLR, potentially leading to estimates of its inclination and ultimately reducing the systematic uncertainties in M_{BH} determinations. In particular, placing direct observational constraints on the value of the reverberation mapping mass scale factor, f (see Onken et al. 2004), even in individual objects, could reduce the scatter in the $M_{\text{BH}}-\sigma_*$ relation for AGNs (Gebhardt et al. 2000; Ferrarese et al. 2001; Onken et al. 2004; Nelson et al. 2004). Despite the diversity in BLR kinematic signatures seen here, we do not see any systematic trends in the location of these objects on the $M_{\text{BH}}-\sigma_*$ relation, suggesting that any effects the different velocity fields of these objects have on their black hole mass estimates are within the current scatter in this relationship. More detailed information about the velocity fields of these objects is needed to say anything further on the effect these kinematic differences have on their black hole mass measurements. Future work will focus on revealing more structure in BLR velocity fields as we

work to create velocity–delay maps of the $H\beta$ emission in NGC 3227, NGC 3516, and NGC 5548 from the data presented here.

We acknowledge support for this work by the National Science Foundation through grant AST-0604066 to The Ohio State University. CMG is grateful for support by the National Science Foundation through grants AST 03-07912 and AST 08-03883. MV acknowledges financial support from HST grants HST-GO-10417, HST-AR-10691, and HST-GO-10833 awarded by the Space Telescope Science Institute, which is operated by the Association of Universities for Research in Astronomy, Inc., for NASA, under contract NAS5-26555. VTD acknowledges the support of the Russian Foundation for Basic Research (project no. 06-02-16843) to the Crimean Laboratory of the Sternberg Astronomical Institute. SGS acknowledges support through Grant No. 5-20 of the "Cosmomicrophysics" program of the National Academy of Sciences of Ukraine to CrAO. The CrAO CCD cameras have been purchased through the US Civilian Research and Development Foundation for the Independent States of the Former Soviet Union (CRDF) awards UP1-2116 and UP1-2549-CR-03. This research has made use of the NASA/IPAC Extragalactic Database (NED) which is operated by the Jet Propulsion Laboratory, California Institute of Technology, under contract with the National Aeronautics and Space Administration and is based on observations obtained at the Dominion Astrophysical Observatory, Herzberg Institute of Astrophysics, National Research Council of Canada.

REFERENCES

- Bentz, M. C., et al. 2006, *ApJ*, 651, 775
— 2008, *ApJ*, 689, L21
— 2009, *ApJ*, submitted, astro-ph/0908.0003
Blandford, R. D., & McKee, C. F. 1982, *ApJ*, 255, 419
Crenshaw, D. M., & Blackwell, Jr., J. H. 1990, *ApJ*, 358, L37
Crenshaw, D. M., Kraemer, S. B., & George, I. M. 2003, *The Observatory*, 123, 57
Davies, R. I., et al. 2006, *ApJ*, 646, 754
Denney, K. D., et al. 2006, *ApJ*, 653, 152
— 2009, *ApJ*, 702, 1353
Done, C., & Krolik, J. H. 1996, *ApJ*, 463, 144
Doroshenko, V. T., Sergeev, S. G., & Pronik, V. I. 2008, *Astronomy Reports*, 52, 442
Eracleous, M., & Halpern, J. P. 1994, *ApJS*, 90, 1
— 2003, *ApJ*, 599, 886
Ferrarese, L., Pogge, R. W., Peterson, B. M., Merritt, D., Wandel, A., & Joseph, C. L. 2001, *ApJ*, 555, L79
Gaskell, C. M. 1988, *ApJ*, 325, 114
Gaskell, C. M., & Goosmann, R. W. 2008, *ApJ*, submitted (astro-ph/0805.4258)
Gebhardt, K., et al. 2000, *ApJ*, 543, L5
Grier, C. J., et al. 2008, *ApJ*, 688, 837
Hicks, E. K. S., & Malkan, M. A. 2008, *ApJS*, 174, 31
Horne, K., Peterson, B. M., Collier, S. J., & Netzer, H. 2004, *PASP*, 116, 465
Kollatschny, W. 2003, *A&A*, 407, 461
Koratkar, A. P., & Gaskell, C. M. 1991, *ApJ*, 375, 85
Murray, N., & Chiang, J. 1997, *ApJ*, 474, 91
Nelson, C. H., Green, R. F., Bower, G., Gebhardt, K., & Weistrop, D. 2004, *ApJ*, 615, 652
Onken, C. A., Ferrarese, L., Merritt, D., Peterson, B. M., Pogge, R. W., Vestergaard, M., & Wandel, A. 2004, *ApJ*, 615, 645
Perez, E., Robinson, A., & de La Fuente, L. 1992, *MNRAS*, 256, 103
Peterson, B. M. 1993, *PASP*, 105, 247
Peterson, B. M. 2001, in *Advanced Lectures on the Starburst-AGN Connection*, ed. I. Aretxaga, D. Kunth, & R. Mújica, 3–+
Peterson, B. M., Wanders, I., Bertram, R., Hunley, J. F., Pogge, R. W., & Wagner, R. M. 1998, *ApJ*, 501, 82
Peterson, B. M., et al. 2004, *ApJ*, 613, 682
Robinson, A., & Perez, E. 1990, *MNRAS*, 244, 138
Rodríguez-Pascual, P. M., et al. 1997, *ApJS*, 110, 9
Sergeev, S. G., Pronik, V. I., Sergeeva, E. A., & Malkov, Y. F. 1999, *ApJS*, 121, 159
Ulrich, M.-H., & Horne, K. 1996, *MNRAS*, 283, 748
Welsh, W. F., & Horne, K. 1991, *ApJ*, 379, 586
Yoshii, Y. 2002, in *New Trends in Theoretical and Observational Cosmology*, ed. K. Sato & T. Shiromizu (Tokyo: Universal Academy), 235
Yoshii, Y., Kobayashi, Y., & Minezaki, T. 2003, in *Bulletin of the American Astronomical Society*, Vol. 35, *Bulletin of the American Astronomical Society*, 752–+